

Cross Platform Alignment (May 2010)

Greg Madejski, *Student, Rochester Institute of Technology*

Abstract—Alignment patterns were exposed using a combination of optical lithography and electron beam lithography. Sub-200nm alignment was achieved by using a combination of silicon topography, global, and fine alignment marks. The average misalignment using this combination was .45 microns. Further work must be done in order to test the efficacy of these alignment marks under different types of thin films.

Index Terms—Electron Beam Lithography, Alignment, Global, Optical Lithography

I. INTRODUCTION

THE purpose of this project is to demonstrate alignment moving from a lithographic platform to an electron beam platform under a scanning electron microscope (SEM). Lithographic steppers have great advantages of processing many wafers quickly and repeatability, but cannot compete with the ultimate resolution capability of electron beam lithography (EBL). However, EBL would never be used for lithography in a manufacturing environment due to the extremely low throughput of exposing individual wafers with direct writing of the feature, compounded with the necessity of performing multiple lithographic steps to create integrated circuits. A compromise between the two platforms could yield the ultimate resolution of EBL with most of the throughput of a lithographic stepper. By using the SEM to expose only the critical layer of lithography (usually the gate length of a transistor), the amount of throughput loss is minimized while the maximum resolution is achieved.

II. THEORY

However, it is not so simple to switch to different exposure processes. In addition to incorporating new photoresists (like polymethylmethacrylate), different problems that are unique to EBL arise. In order to migrate to a new exposure platform, a common reference must be created so that the product can move from the lithographic stepper to the SEM and back again. This was achieved by using a 0th level alignment mark that is included on every mask used for the specific lithographic stepper in question at RIT. This mark could be then used for global alignment across the die, where fine alignment marks then could be used for individual feature alignment. Figure 1 shows the topography of one of these fine alignment marks.

Another problem is evident as the electron beam is scanned across the sample surface, and read by the EBL exposure software. Image skewing is observed when the imaging hardware doesn't have enough time to discharge when reading a sample signal from the SEM. This makes alignment difficult, as the image topography does not precisely mirror what was present

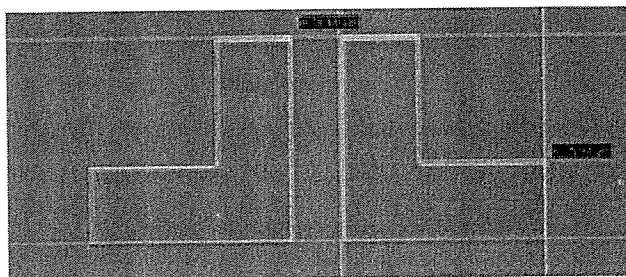


Fig. 1. SEM Micrograph image of fine alignment elbows. The contrast is created by silicon topography, where the elbows are 608nm tall mesas.

on the surface. A longer time to scan the sample surface mitigates the worst of this skew, allowing the hardware more time to discharge. Figure 2 demonstrates this phenomenon, comparing a normal SEM micrograph of the global alignment mark compared to the same mark as viewed through the pattern recognition software.

III. EXPERIMENTAL PROCEDURE AND OBSERVATIONS

In order to test these issues, a 0th level mask was patterned on a silicon substrate using a GCA 6700 g-line stepper. This pattern, along with subsequent alignment mark, was etched into the silicon using a Trion Reactive Ion Etcher (RIE) in a CF₄ and O₂ ambient for 225 seconds, creating mesa features 608 nm high. The alignment features were examined under a LEO 1530 SEM, after the substrate had been cleaved into pieces. Images of the GCA global alignment mark and the fine alignment elbows were taken as various noise reduction techniques were applied to the image, including line-integration and frame averaging. A PMMA based photoresist was applied to one etched piece and exposed on the LEO 1530 SEM, after dummy alignment features had been created in DesignCAD software for a 1st level alignment. NPGS software was used to create and process a runfile that varied the type of alignment in 4 rows of 5 subfields, where the first row had both manual global and fine alignment marks in each subfield, the second and third rows had only manual global alignment at the start of each row, and the fourth row had global alignment, but only one fine alignment at the first subfield. Figure 3 shows the procedure.

IV. RESULTS AND DISCUSSION

Figures 4 and 6 show the results of the 1st level alignment. Qualitatively, the first row had the best alignment overall, including two subfields that were perfectly aligned, followed by the fourth row that had gradually become misaligned across the row. The second and third rows showed the most misalignment, off by as much as 5 μm in either orientation. The

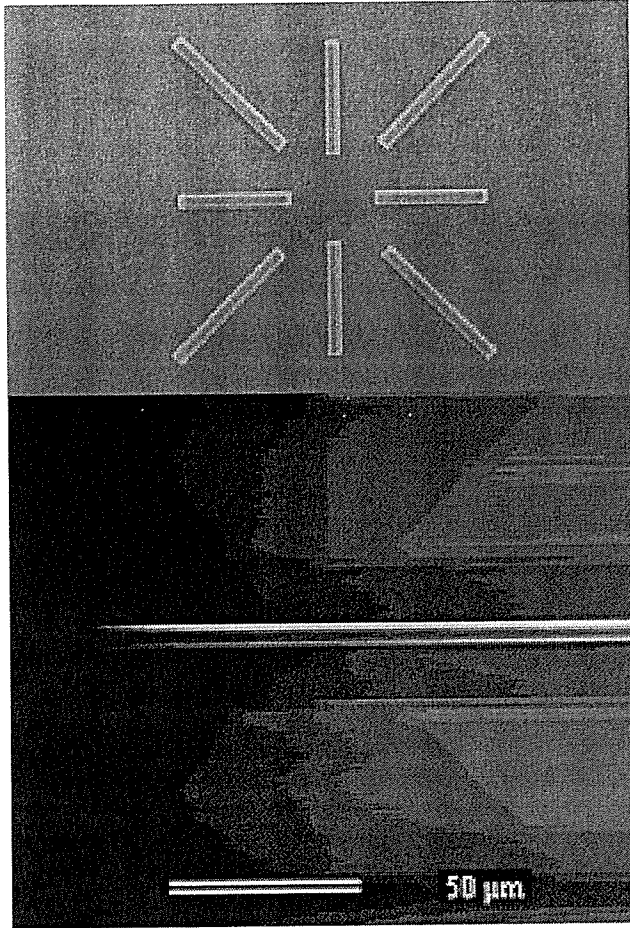


Fig. 2. Top: SEM micrograph of GCA alignment mark, used for global alignment, raised as 608nm mesa. Bottom: GCA alignment mark imaged into pattern recognition software, displaying image skew, as the electron beam is rastered across the feature. Slower scan speeds of the beam produced less skew.

Experimental Setup

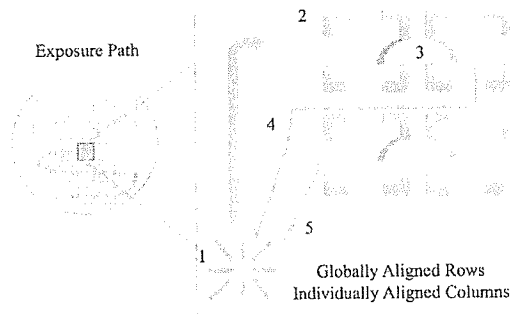


Fig. 3. Experimental Exposure. (1) Global alignment is performed (2) Fine alignment is performed on all corners (3) Die are completed until the end of the row (4) Global alignment is performed again (5) Steps 2-4 repeat.

horizontal alignment was the most variant overall, showing an oscillatory trend. The global alignment mark was much

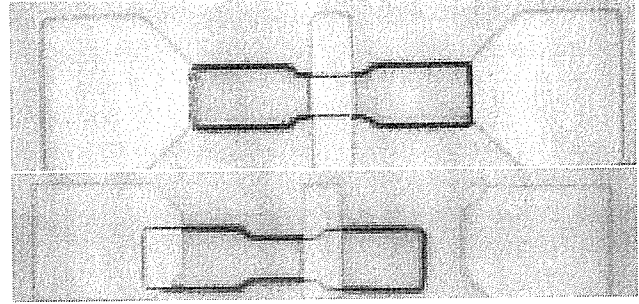


Fig. 4. Top: 1000x image of alignment pattern overlaid from manual alignments of both global and fine-feature marks. The misalignment is negligible. Bottom: 1000x image of alignment pattern imperfectly aligned based on manual alignment of global alignment mark, $\delta x = +4.2 \mu\text{m}$, $\delta y = +1.6 \mu\text{m}$. Misalignment ranged up to $5 \mu\text{m}$ for both orientations, over 20 different exposures.

easier to align to than the fine alignment elbows due to the greater size of the global feature, as well as having diagonal orientations as reference. Based on these results, an optimized mask template has been created, taking into account the need for an easy-to-use coordinate system, subfield arrays, both fine and global alignment marks, and a quick read of the alignment accuracy. Figure 5 shows the template diagram.

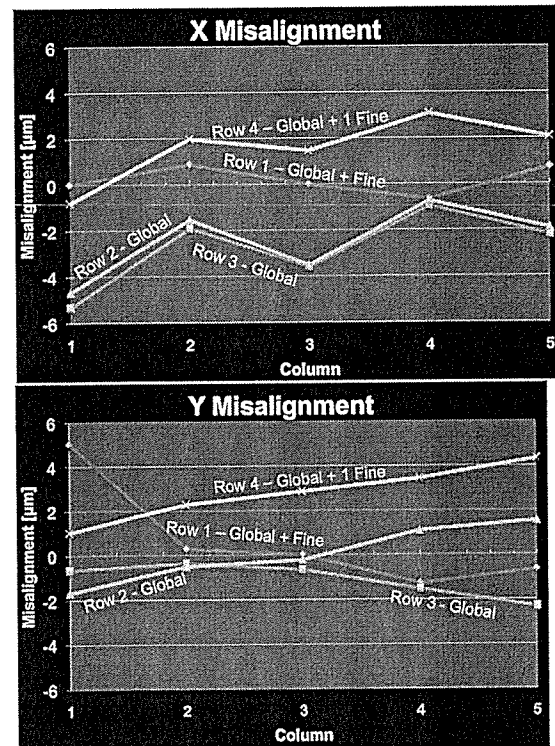


Fig. 5. Experimental horizontal alignment results based on 3 different alignment methodologies. Global alignment on Rows 2 and 3 resulted in an average misalignment of $2.6 \mu\text{m}$, while the average misalignment for Row 1 was $0.45 \mu\text{m}$. Average misalignment for Row 4 was $1.87 \mu\text{m}$. Bottom: Experimental vertical alignment results. The best alignment exposure occurred on Row 1, Column 3, where both global and fine alignment occurred.

HotPlot v2009.1.1.1
 Submitted by user: gmn0189 from node vlsi-30 on Wed May 5 12:30:25 2010
 Library -- H Cell -- 50 design template task Setup -- setup.p Strip 1 of 1
 Bounds -- LL: -2875.00, -1375.00, LR: 2875.00, 1375.00 Mag -- 29.84 Angle -- 0
 Layer information -- 1k 43k 46k 47k 49k 51k

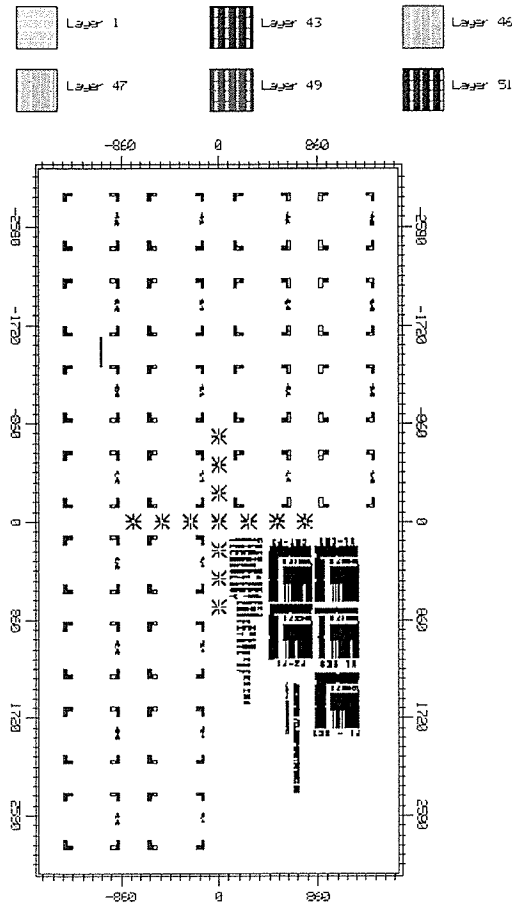


Fig. 6. Sample Template Mask Layout

V. CONCLUSIONS

Ultimately, it is possible to align EBL to optical lithography's resultant topography. Alignment error can be negligible with global and fine alignment, but takes a relatively large amount of time to achieve (approximately 2 minutes per subfield). A sample mask layout has been created for future users' ease.

VI. ACKNOWLEDGMENTS

The author would like to thank David Pawlik, Paul Thomas, Mike Barth, Robert Brown, Ken Nagamatsu, and Dr. Rommel for assistance with this work.